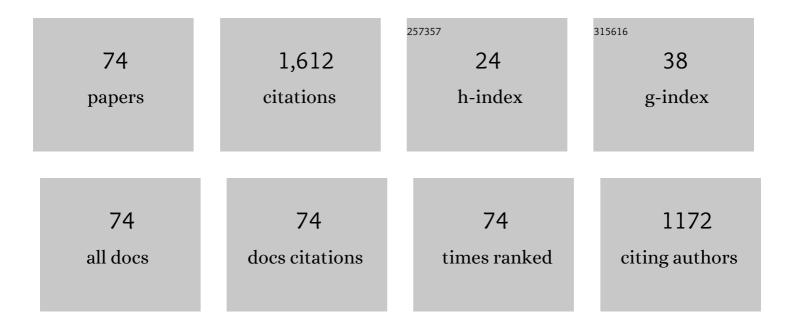
## Ida Lykke Fabricius

List of Publications by Year in descending order

Source: https://exaly.com/author-pdf/4929372/publications.pdf Version: 2024-02-01



#	Article	IF	CITATIONS
1	How burial diagenesis of chalk sediments controls sonic velocity and porosity. AAPG Bulletin, 2003, 87, 1755-1778.	0.7	119
2	Stylolites, porosity, depositional texture, and silicates in chalk facies sediments. Ontong Java Plateau ? Gorm and Tyra fields, North Sea. Sedimentology, 2007, 54, 183-205.	1.6	93
3	Chalk: composition, diagenesis and physical properties. Bulletin of the Geological Society of Denmark, 2007, 55, 97-128.	1.1	93
4	Different effects of temperature and salinity on permeability reduction by fines migration in Berea sandstone. Geothermics, 2015, 53, 225-235.	1.5	85
5	Permeability in Rotliegend gas sandstones to gas and brine as predicted from NMR, mercury injection and image analysis. Marine and Petroleum Geology, 2015, 64, 189-202.	1.5	76
6	The effect of hot water injection on sandstone permeability. Geothermics, 2014, 50, 155-166.	1.5	71
7	Petrophysical and rock-mechanics effects of CO2 injection for enhanced oil recovery: Experimental study on chalk from South Arne field, North Sea. Journal of Petroleum Science and Engineering, 2014, 122, 468-487.	2.1	59
8	How depositional texture and diagenesis control petrophysical and elastic properties of samples from five North Sea chalk fields. Petroleum Geoscience, 2007, 13, 81-95.	0.9	56
9	Elastic moduli of dry and water-saturated carbonates — Effect of depositional texture, porosity, and permeability. Geophysics, 2010, 75, N65-N78.	1.4	56
10	Chemical and mechanical processes during burial diagenesis of chalk: an interpretation based on specific surface data of deep-sea sediments. Sedimentology, 1998, 45, 755-769.	1.6	55
11	Chalk porosity and sonic velocity versus burial depth: Influence of fluid pressure, hydrocarbons, and mineralogy. AAPG Bulletin, 2008, 92, 201-223.	0.7	51
12	Biot's coefficient as an indicator of strength and porosity reduction: Calcareous sediments from Kerguelen Plateau. Journal of Petroleum Science and Engineering, 2010, 70, 282-297.	2.1	51
13	Petrophysical properties of greensand as predicted from NMR measurements. Petroleum Geoscience, 2011, 17, 111-125.	0.9	48
14	New insight into the microtexture of chalks from NMR analysis. Marine and Petroleum Geology, 2016, 75, 252-271.	1.5	45
15	Estimating permeability of carbonate rocks from porosity and vp â^• vs. Geophysics, 2007, 72, E185-E191.	1.4	41
16	Permeability, compressibility and porosity of Jurassic shale from the Norwegian–Danish Basin. Petroleum Geoscience, 2014, 20, 257-281.	0.9	35
17	Static and dynamic effective stress coefficient of chalk. Geophysics, 2012, 77, L1-L11.	1.4	34
18	<i>V<sub>p</sub>â€V<sub>s</sub></i> relationship and amplitude variation with offset modelling of glauconitic greensand <sup>â€i</sup> . Geophysical Prospecting, 2012, 60, 117-137.	1.0	30

IDA LYKKE FABRICIUS

#	Article	IF	CITATIONS
19	Static and dynamic Young's moduli of chalk from the North Sea. Geophysics, 2008, 73, E41-E50.	1.4	29
20	Prediction of Archie's cementation factor from porosity and permeability through specific surface. Geophysics, 2008, 73, E81-E87.	1.4	27
21	Influence of porosity and pore fluid on acoustic properties of chalk: AVO response from oil, South Arne Field, North Sea. Petroleum Geoscience, 2004, 10, 319-330.	0.9	26
22	Modelling elastic properties of impure chalk from South Arne Field, North Sea. Geophysical Prospecting, 2007, 55, 487-506.	1.0	26
23	Sensitivity analysis of recovery efficiency in high-temperature aquifer thermal energy storage with single well. Energy, 2015, 90, 1349-1359.	4.5	25
24	Grain size distributions of chalk from image analysis of electron micrographs. Computers and Geosciences, 2001, 27, 1071-1080.	2.0	24
25	Burial stress and elastic strain of carbonate rocks. Geophysical Prospecting, 2014, 62, 1327-1336.	1.0	22
26	Caprock compressibility and permeability and the consequences for pressure development in CO2 storage sites. International Journal of Greenhouse Gas Control, 2014, 22, 139-153.	2.3	22
27	Biot critical frequency applied to description of failure and yield of highly porous chalk with different pore fluids. Geophysics, 2010, 75, E205-E213.	1.4	20
28	Interpretation of Water Saturation Above the Transitional Zone in Chalk Reservoirs. SPE Reservoir Evaluation and Engineering, 2004, 7, 155-163.	1.1	19
29	Incorporating electrostatic effects into the effective stress relation — Insights from chalk experiments. Geophysics, 2018, 83, MR123-MR135.	1.4	19
30	Phosphate removal by iron oxide-coated diatomite: Laboratory test of a new method for cleaning drainage water. Chemosphere, 2019, 222, 884-890.	4.2	19
31	Rock physics model of glauconitic greensand from the North Sea. Geophysics, 2011, 76, E199-E209.	1.4	18
32	Permeability prediction in chalks. AAPG Bulletin, 2011, 95, 1991-2014.	0.7	17
33	Prediction of Biot's coefficient from rock-physical modeling of North Sea chalk. Geophysics, 2008, 73, E89-E96.	1.4	16
34	The effect of divalent ions on the elasticity and pore collapse of chalk evaluated from compressional wave velocity and low-field Nuclear Magnetic Resonance (NMR). Journal of Petroleum Science and Engineering, 2015, 136, 88-99.	2.1	13
35	Comparative analysis of experimental methods for quantification of small amounts of oil in water. Journal of Petroleum Science and Engineering, 2016, 147, 459-467.	2.1	12
36	Methods of velocity prediction tested for North Sea chalk: a review of fluid substitution and vS estimates. Journal of Petroleum Science and Engineering, 2004, 45, 129-139.	2.1	10

IDA LYKKE FABRICIUS

#	Article	IF	CITATIONS
37	Elastic and nonelastic deformation of greensand. The Leading Edge, 2009, 28, 86-88.	0.4	10
38	Production of Calcareous Nannofossil Ooze For Sedimentological Experiments. Journal of Sedimentary Research, 2015, 85, 1228-1237.	0.8	10
39	Thermal conductivity of sandstones from Biot's coefficient. Geophysics, 2018, 83, D173-D185.	1.4	10
40	Low field NMR surface relaxivity studies of chalk and argillaceous sandstones. Microporous and Mesoporous Materials, 2018, 269, 122-124.	2.2	9
41	Porosity in chalk – roles of elastic strain and plastic strain. Sedimentology, 2020, 67, 3451-3470.	1.6	9
42	Core Flooding Experiments and Reactive Transport Modeling of Seasonal Heat Storage in the Hot Deep Gassum Sandstone Formation. ACS Earth and Space Chemistry, 2017, 1, 251-260.	1.2	8
43	Effective stresses and shear failure pressure from in situ Biot's coefficient, Hejre Field, North Sea. Geophysical Prospecting, 2017, 65, 808-822.	1.0	8
44	Effect of Temperature on Stiffness of Sandstones from the Deep North Sea Basin. Rock Mechanics and Rock Engineering, 2021, 54, 255-288.	2.6	8
45	Flow characterization of glauconitic sandstones by integrated Dynamic Neutron Radiography and image analysis of backscattered electron micrographs. Petroleum Geoscience, 2003, 9, 175-183.	0.9	7
46	Surface charge of calcite and its influence on the electrical conductivity in chalk. , 2010, , .		7
47	Equivalent pore radius and velocity of elastic waves in shale. Skjold Flank-1 Well, Danish North Sea. Journal of Petroleum Science and Engineering, 2013, 109, 280-290.	2.1	7
48	A mechanism for water weakening of elastic moduli and mechanical strength of chalk. , 2010, , .		7
49	Modeling of the pressure propagation due to CO 2 injection and the effect of fault permeability in a case study of the Vedsted structure, Northern Denmark. International Journal of Greenhouse Gas Control, 2014, 28, 1-10.	2.3	6
50	Water weakening of elastic moduli of carbonates interpreted by use of isoâ€frame modeling. , 2008, , .		5
51	Injection of Ca-depleted formation water in the Lower Triassic Bunter Sandstone Formation for seasonal heat storage in geothermal sandstone reservoirs: Effects on reservoir quality. Geothermics, 2021, 96, 102179.	1.5	5
52	Determination of Matrix Pore Size Distribution in Fractured Clayey Till and Assessment of Matrix Migration of Dechlorinating Bacteria. Bioremediation Journal, 2014, 18, 295-308.	1.0	4
53	Effect of electrostatic forces on the porosity of saturated mineral powder samples and implications for chalk strength. Geophysics, 2020, 85, MR37-MR50.	1.4	4
54	Rock physics model of glauconitic greensand from the North Sea. , 2010, , .		4

4

IDA LYKKE FABRICIUS

#	Article	IF	CITATIONS
55	Waterâ€flooding and consolidation of reservoir chalk – effect on porosity and Biot's coefficient. Geophysical Prospecting, 2021, 69, 495-513.	1.0	3
56	The feasibility of high-temperature aquifer thermal energy storage in Denmark: the Gassum Formation in the Stenlille structure. Bulletin of the Geological Society of Denmark, 0, 68, 133-154.	1.1	3
57	Dispersion of elastic waves in carbonate rocks , 2009, , .		2
58	Clay squirt: Local flow dispersion in shale-bearing sandstones. Geophysics, 2017, 82, MR51-MR63.	1.4	2
59	Water weakening of soft and stiff outcrop chalk induced by electrical double layer disjoining pressure. International Journal of Rock Mechanics and Minings Sciences, 2021, 141, 104700.	2.6	2
60	Change in Biot's Effective Stress Coefficient of Chalk During Pore Collapse. , 2013, , .		1
61	Porosity and sonic velocity depth trends of Eocene chalk in Atlantic Ocean: Influence of effective stress and temperature. Journal of Petroleum Science and Engineering, 2014, 122, 216-229.	2.1	1
62	Fluid substitution in sandstone: Effective porosity or total porosity. , 2015, , .		1
63	Permeability Estimation in Chalk Using NMR and a Modified Kozeny Equation. , 2017, , .		1
64	Elasticity and Density of Paleozoic Shales from Bornholm. , 2017, , .		1
65	Stratigraphy and petrophysical characteristics of Lower Paleocene cool-water carbonates, Faxe quarry, Denmark. Bulletin of the Geological Society of Denmark, 0, 69, 97-121.	1.1	1
66	Influence of pore fluid and frequency on elastic properties of greensand as interpreted using NMR data. , 2011, , .		1
67	Effect of dissolved ions on bound water on water wet mineral surfaces as indicated by NMR transverse relaxation time (T2). , 2013, , .		1
68	Interpretational challenges related to studies of chalk particle surfaces in scanning and transmission electron microscopy. Bulletin of the Geological Society of Denmark, 2018, 66, 151-165.	1.1	1
69	Relation of acoustic impedance to stiffness and porosity of Maastrichtian chalk in Dan field, Danish North Sea. Geophysical Prospecting, 0, , .	1.0	1
70	Biot Critical Frequency Applied as Common Friction Factor for Pore Collapse and Failure of Chalk With Different Pore Fluids and Temperatures. SPE Journal, 2011, 16, 1002-1009.	1.7	0
71	The effect of brine saturation on the elastic moduli of compacted clay. , 2015, , .		0
72	How Pore Filling Shale Affects Elastic Wave Velocities in Fully and Partially Saturated Sandstone: Characterization, Measurement, and Modelling. , 2017, , .		0

#	Article	IF	CITATIONS
73	Elastic moduli of sandstones saturated with a range of pore fluids correlated with kinematic viscosity and frequency ratio. , 2011, , .		0
74	Effective stress on deep sedimentary formations under nonisothermal conditions. , 2018, , .		0